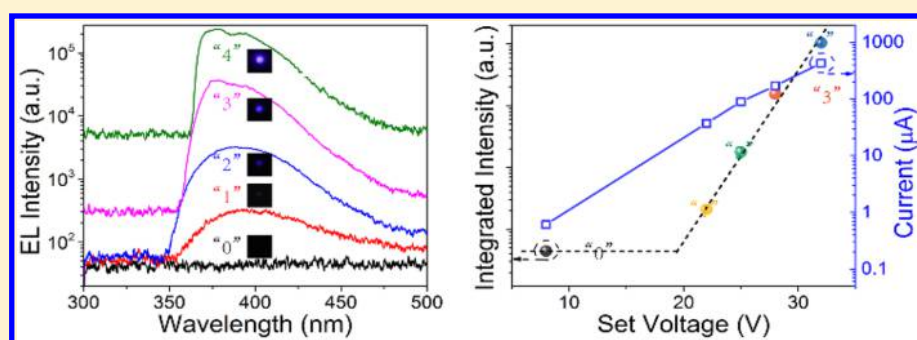


Light-Emitting Devices Modulated by Multilevel Resistive Memories

Xun Yang,^{†,‡} Chongxin Shan,^{*,†,‡,§} Qi Liu,[§] Mingming Jiang,^{†,§} Yingjie Lu,[‡] Xiuhua Xie,[†] Binghui Li,[†] and Dezhen Shen^{*,†}[†]State Key Laboratory of Luminescence and Applications, Changchun Institute of Optics, Fine Mechanics and Physics, Chinese Academy of Sciences, Changchun 130033, China[‡]School of Physics and Engineering, Zhengzhou University, Zhengzhou 450052, China[§]Key Laboratory of Microelectronic Devices & Integrated Technology, Institute of Microelectronics, Chinese Academy of Sciences, Beijing 100029, China

Supporting Information



ABSTRACT: We demonstrate for the first time that multilevel resistive random access memories (RRAMs) can be utilized to modulate the luminescence of light-emitting devices (LEDs) in Au/GaO_x/p-GaN/n-ZnO structures. In these structures, Au/GaO_x/p-GaN multilevel RRAMs are integrated with p-GaN/n-ZnO LEDs. The injection current of the LEDs can be controlled by the resistance states of the multilevel RRAMs, thus modulating the luminous intensity. The results reported in this paper may offer a route to more integrated and low-cost LED displays. Moreover, our approach may provide a clue for the diversified applications by integrating RRAMs with other functional electronics.

KEYWORDS: light-emitting devices, resistive random access memories, multilevel switching

In the past decades, light-emitting devices (LEDs) have attracted much attention for their significance in both fundamental research and practical applications in the field of displaying, lighting, labeling, and so on due to their advantages of high brightness, high efficiency, and long lifetime.^{1–10} For the technological applications of displays, the on/off state and gray scale of each pixel are controlled by external thin film transistor (TFT) or complementary metal-oxide-semiconductor (CMOS) via modulating the injection current, which are constructed by complicated fabrication techniques.^{11–14} If the number of transistors and circuit complexity could be reduced, more integrated and low-cost LED display panels may be achieved. Due to their multilevel switching characteristics and simple structure, resistive random access memories (RRAMs) may be a promising way to modulate the driving current applied on LED pixels.^{15–18} In general, an RRAM memory is composed of a metal–insulator–metal (MIM) sandwich structure or a Schottky junction.¹⁹ The underlying mechanism behind RRAMs is resistive switching.^{20–22} Meanwhile, multilevel RRAMs, in which multilevel resistance states (RSs) are achieved by means of different set voltages (V_{set}), may be utilized to modulate the driving current applied onto the LED pixels, thus, realizing on/off state and gray scale by modulating

the luminous intensity of the LEDs. However, none such report can be found to date.

In this study, we demonstrate that the luminous intensity of LEDs can be modulated by multilevel RRAMs for the first time, and the RRAMs modulated LEDs were realized in Au/GaO_x/p-GaN/n-ZnO structures. In these structures, the p-GaN/n-ZnO junctions act as LEDs that can produce strong emission at current injection, and the Au/GaO_x/p-GaN junctions act as driving current controllers to modulate the luminous intensity of the LEDs. The multilevel switching behavior of the Au/GaO_x/p-GaN junctions originates from the variation of Schottky barrier due to the charge trapping/detrapping process. By modulating the RSs of the Au/GaO_x/p-GaN junction RRAMs via various V_{set} , multilevel luminous states have been achieved from the LEDs. In these devices, multilevel RRAMs have been integrated with LEDs to modulate the luminous intensity, replacing complicated driving transistors in each pixel circuit, which may be a promising way toward more integrated and low-cost LED displays.

Received: November 2, 2017

Published: December 5, 2017

Figure 1a shows the schematic diagram of the Au/GaO_x/p-GaN/n-ZnO structure, and the existence of the GaO_x layer at

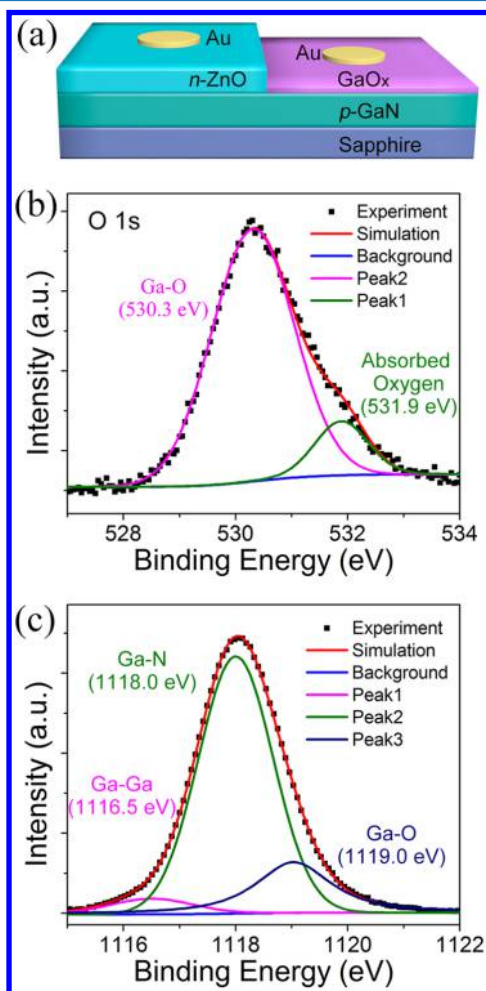


Figure 1. (a) Schematic diagram of the Au/GaO_x/p-GaN/n-ZnO structure; XPS spectra of the O 1s (b) and Ga 2p_{3/2} (c) peak for the GaN surface after annealed in O₂ ambient at 650 °C for 30 min.

the surface of the GaN has been confirmed by XPS analysis. Two peaks can be observed from the O 1s XPS spectra of the GaN surface (Figure 1b), which can be attributed to Ga–O bonding (530.3 eV) and nonlattice oxygen ions (531.9 eV).^{18,23,24} The XPS spectra of Ga 2p_{3/2} in Figure 1c shows three peaks, which can be attributed to Ga–Ga bonding (1116.5 eV), Ga–N bonding (1118.0 eV) and Ga–O bonding (1119.0 eV).^{23,25,26} In this structure, the Au/GaO_x/p-GaN multilevel RRAM acts as a driving current controller and the p-GaN/n-ZnO performs as a luminescent device. Although resistive switching effect has also been reported from ZnO films, but in our case, it cannot be observed from the ZnO film as the *I*–*V* curve of the p-GaN/n-ZnO junction shows no switching behavior (see Supporting Information, Figure S1).

Figure 2a shows the resistive switching characteristics of the Au/GaO_x/p-GaN/n-ZnO structure, in which forward bias is defined as the situation that positive bias is applied onto the Au electrode on the GaO_x/p-GaN junction. The arrows in the figure denote the voltage sweeping direction. Initially, the device is in a high resistance state (HRS, OFF state). As the voltage sweeps from 0 to +30 V (sweep 1), the current increases rapidly once the voltage exceeds a specific voltage,

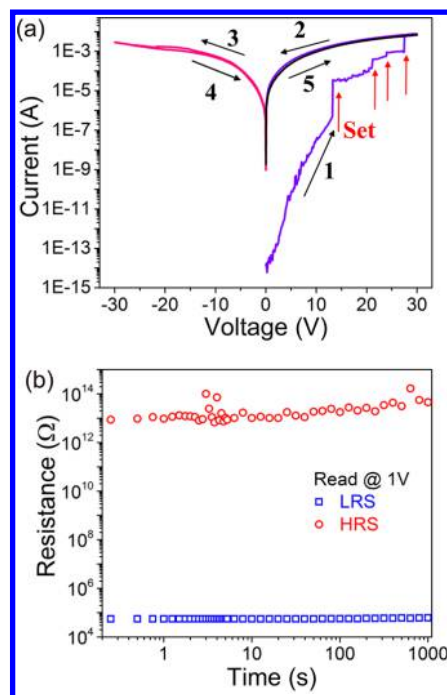


Figure 2. (a) *I*–*V* characteristics of the Au/GaO_x/p-GaN/n-ZnO structure; (b) Retention test at a reading voltage of +1 V in LRS/HRS state.

equivalent to a SET process. As the voltage goes on sweeping to +30 V, several other rapid increases in the current flow can be observed. The multilevel SET process before the device reaches its final low resistance state (LRS, ON state) indicates the presence of more inherent RSs between the LRS and HRS. The LRS is maintained in the following sweep 2 (from +30 to 0 V), indicating the nonvolatile feature of the device. When negative voltage is applied onto the device, the resistance increases only slightly (sweep 3 and 4). The stability of the switching is also an important factor for memories. To test the stability of the structure, the HRS/LRS state was probed at regular time intervals using a +1 V bias as reading voltage, as shown in Figure 2b. During the measurement, the resistance of the LRS maintains 8 orders of magnitude smaller than that of the HRS. A retention time of around 1000 s has been obtained. The multi RSs and good stability of the device suggest that multilevel RRAMs may be utilized to modulate the injection current of LEDs. Moreover, the high ON/OFF resistance ratio of $\sim 10^8$ ensures the distinctiveness of each neighboring state.

Conducting filaments and charge trapping/detrapping are two main mechanisms that have been demonstrated to be responsible for the resistive switching behaviors.^{19,27–30} To explore the switching mechanism in our case, the *I*–*V* characteristics of the Au/GaO_x/p-GaN/n-ZnO structure have been investigated, as shown in Figure 3a. HRS *I*–*V* curve shows prominent rectifying behavior, which can be attributed to the Au/GaO_x/p-GaN Schottky junction.^{31–34} Note that although rectifying behavior also exists in the p-GaN/n-ZnO junction, the opening direction of the p-GaN/n-ZnO junction is opposite to that of the Au/GaO_x/p-GaN Schottky junction, and the current injection under positive bias is mainly limited by the reversely biased Schottky junction, supporting the Schottky emission mechanism. Moreover, the decrease of current in ON state also serves as an evidence for the validity of the charge trapping/detrapping mechanism, as shown in Figure 3b.^{19,28}

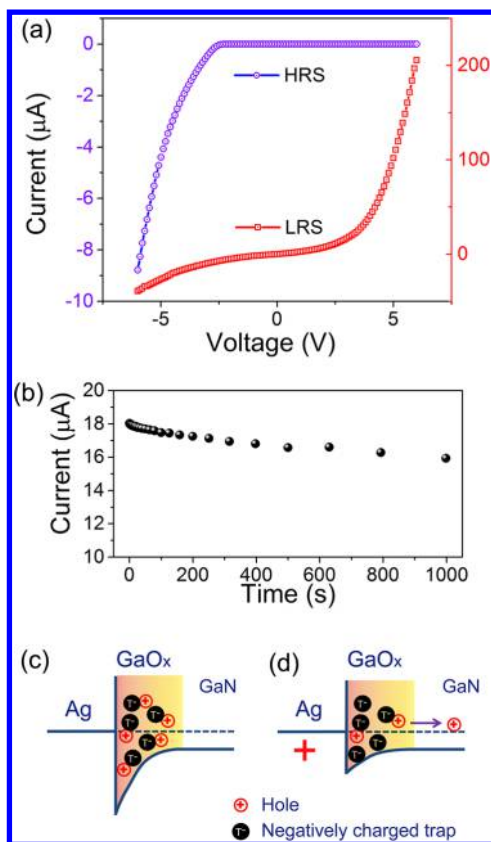


Figure 3. (a) I - V behaviors of the HRS and LRS of the Au/GaO_x/ p -GaN/ n -ZnO structure; (b) The decrease of current in LRS state read at +1 V; Schematic band diagram of the HRS (c) and LRS (d) of the Au/GaO_x/ p -GaN junction. The hole detrapping causes the reduced barrier height and forms switches to the LRS.

The switching mechanism of the device can be understood in the schematic bandgap diagram of the Au/GaO_x/ p -GaN Schottky junction, as indicated in Figure 3c. Initially, due to the thin GaO_x layer, the Schottky barrier in the Au/GaO_x/ p -GaN is high.^{31,35} Under positive bias, the Schottky barrier limits the current flow and the device is in HRS. In the GaO_x layer, there exist trapping states such as defects and impurity states. Upon the high voltage drop across the reversely biased Schottky barrier, some trapped holes in the GaO_x layer will be detrapped and flow toward p -GaN, leaving negatively charged empty traps nearby the interface, as shown in Figure 3d.^{29,31,36} The negatively charged traps change the potential distribution within the depletion region, which will lower the Schottky barrier and turn the device into LRS. Memories based on the charge trapping/detrapping effects are usually reversible. Whereas, in our case, the resistance only increases slightly under reverse bias, this is because of the fact that the barrier in the Au/GaO_x/ p -GaN Schottky junction is low in ON state, thus reverse bias is mostly applied onto the series resistance of the GaN, which means that the bias distributed to the Au/GaO_x/ p -GaN junction is not high enough to reset it back into the original HRS.

It has been shown that multilevel RSs can be achieved by varying the compliance current or V_{set} . Due to the multilevel SET process before the device reaches its final LRS, multiple LRSs can be achieved by means of varying V_{set} . By sweeping the applied voltage from 0 to 10 V, the RS is switched to LRS1 from the HRS. In the subsequent sweep, the V_{set} are applied to higher voltages of 15, 25, and 35 V from 0 V, and lower RSs LRS2, LRS3, and LRS4 are subsequently achieved, as shown in Figure 4a. The retention time of each RS tested by a periodical 1 V pulse is more than 1000 s, as shown in Figure 4b.

To further verify whether the resistive switching is induced by the variation of Schottky barrier, we studied the Schottky

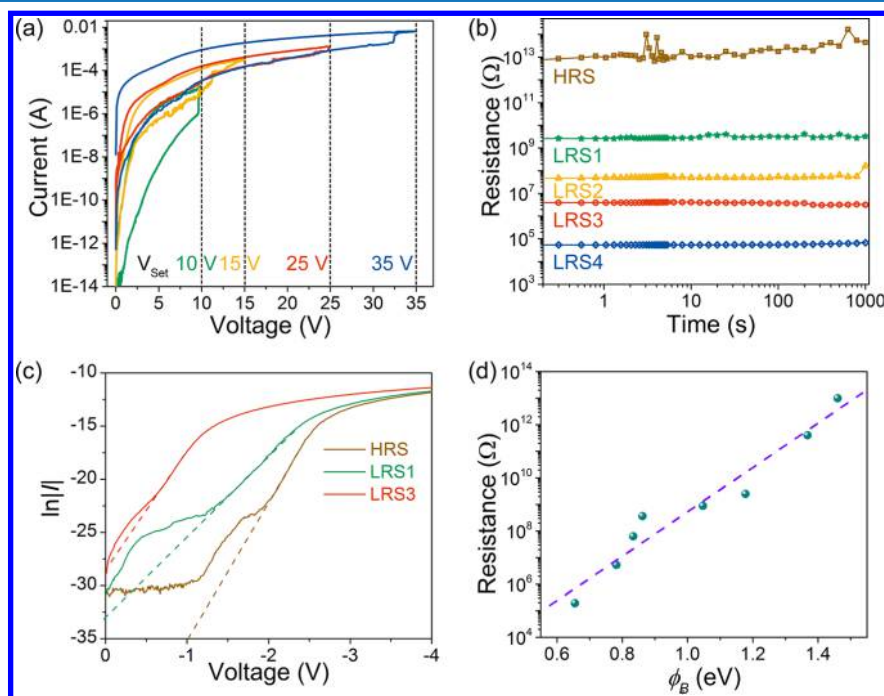


Figure 4. (a) I - V characteristics of the Au/GaO_x/ p -GaN/ n -ZnO structure at different set stop voltages (10, 15, 25, and 35 V in sequence) (b) The retention of each state in around 1000 s. (c) I - V characteristics of the Au/GaO_x/ p -GaN/ n -ZnO structure in different RSs. The dashed lines are fits to the thermionic emission process. (d) The relationship between the resistance and the deduced barrier height.

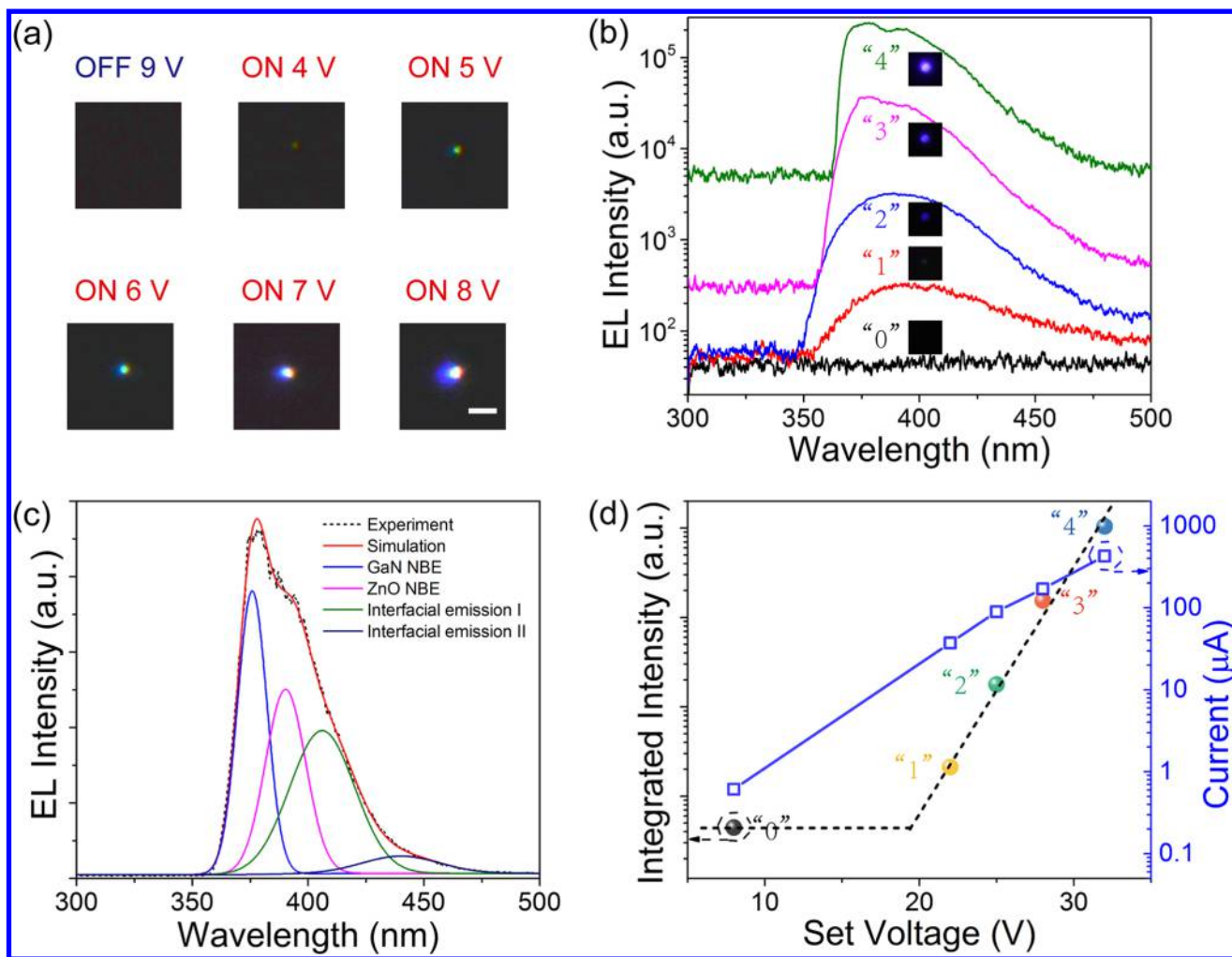


Figure 5. (a) Optical images of the Au/GaO_x/p-GaN/n-ZnO structure in ON/OFF state as a function of reading voltage; (b) EL spectra and optical images of the device in different luminous states at reading voltage of +8 V. The device is set into different luminous states by applying various V_{set} (8, 22, 25, 28, and 32 V), the current is 0.61, 37, 89, 170, and 425 μA , respectively. (c) Gaussian fit of the EL spectrum of luminous state "3". (d) The variation of injection current and luminous intensity vs V_{set} .

barrier of each RS. Taking the standard Schottky barrier model into account, the current under forward bias can be determined by applied bias according to the following expression:³¹

$$I = J_0 S \exp\left(\frac{eV}{n}\right) \quad (1)$$

$$J_0 = A^* T^2 \exp\left(-\frac{e\phi_B}{k_B T}\right) \quad (2)$$

where S is the junction area, e is the electron charge, n is the ideality factor, k_B is the Boltzmann's constant, T is the temperature, A^* is Richardson's constant, and ϕ_B is the Schottky barrier height. It is expected that, in higher voltage region prior to the saturation of current due to series Ohmic resistance, the current increases exponentially with voltage. Figure 4c shows $\ln I$ - V curves in HRS, LRS1, and LRS3, which fit well with the straight dashed lines. The deviation of the $\ln I$ - V curves from the linear fitting at lower voltage may come from excess current flows through the Schottky barrier.³¹ The value of ϕ_B can be deduced from the intercept of the linear part of the $\ln I$ - V plot at $V = 0$. Figure 4d shows the relationship between the obtained ϕ_B and the resistance at +1 V, an approximate linear relationship between $\log R$ and ϕ_B can be

observed, confirming that the resistive switching is originated from the variation of the Schottky barrier.

To investigate the feasibility of utilizing the multilevel switching memories to modulate the luminous intensity of the LEDs, the emission characteristics of the device have been studied using +8 V as reading voltage. +8 V is chosen as the reading voltage because it is large enough to induce luminescence brightly in LRS (Figure 5a) but smaller than the lowest switching voltage (9.6 V, see Figure 4a). Various V_{set} have been employed to modulate the luminous intensity by tuning the injection current. Initially, the device is in HRS and the current at +8 V is 0.61 μA , no emission can be observed from the LED (Figure 5b) due to the low current injection. The V_{set} is denoted as +8 V and the luminous state as "0" for clarity. After subsequently applied by V_{set} of 22, 25, 28, and 32 V, the injection current is tuned to 37, 89, 170, and 425 μA accordingly, obvious emission with different luminous intensity can be observed from the spectra and optical images, as indicated in Figure 5b. The device has been set into different luminous states denoted as "1", "2", "3", and "4". All the luminous states show good stability during a 1000 s retention test (see Supporting Information, Figure S2). One can see that for all the luminous states, the emission spectra are asymmetric.

And each spectrum can be fitted well using four Gaussian peaks at 375.8, 390.2, 406.0, and 440.0 nm, as shown in Figure 5c. The peaks at 375.8 and 390.2 nm can be attributed to NBE emissions of GaN and ZnO, respectively, and the other two peaks can be attributed to interfacial emissions.^{37–40} The variation of luminous intensity and injection current as a function of V_{set} has also been studied, as shown in Figure 5d. It should be noted that the injection current in logarithmic coordinate increases with V_{set} , whereas the luminescence maintains OFF until V_{set} reaches a certain value (about 19 V), as denoted by the dashed line, because the related current must reach a threshold before luminescence occurs. Then the logarithm of luminous intensity increases approximately linearly.

Based on the above facts, multilevel RRAMs have been utilized to modulate the injection current and luminous intensity of LEDs for the first time. In this design, the current controller and the LED have been integrated into one device, performing as a display pixel. Thus, the circuit complexity can be reduced greatly. In principle, more luminous states could be generated by employing more V_{set} due to the continuous variation in Schottky barrier, satisfying the practical application requirements of LED displays. Moreover, the issue that the RRAMs cannot be switched to HRL from LRS can be solved using three-dimensional structure, which will reduce the voltage applied onto series resistance under reversed bias.

In summary, multilevel RRAMs have been integrated with LEDs to modulate the luminescence of LEDs for the first time in Au/GaO_x/p-GaN/n-ZnO structures. In this design, the multilevel switching behaviors stem from the variation of barrier in the Au/GaO_x/p-GaN Schottky junction. The results reported in this paper may offer a route to LED displays avoiding the complicated fabrication process of driving transistor in the future. In addition, our approach may provide a clue for the diversified applications by integrating RRAMs with other functional electronics.

EXPERIMENTAL SECTION

The Mg-doped *p*-type GaN layer was grown on *c*-plane sapphire by molecular beam epitaxy (MBE) with an undoped GaN layer as the buffer layer. The precursors used for the growth and doping of GaN were elemental gallium and magnesium, and the N₂ gas employed as the nitrogen source for GaN was activated by an Oxford Applied Research HD25 radio frequency plasma cell. During the growth process of the *p*-GaN, the temperature of Ga source and Mg source were fixed at 1135 and 340 °C, respectively. The substrate temperature was kept at 900 °C, and the N₂ flow rate was maintained at 3.34 sccm. The thickness of the grown *p*-GaN is about 1.3 μm, and the hole concentration and Hall mobility are $5.3 \times 10^{17} \text{ cm}^{-3}$ and $1.7 \text{ cm}^2 \text{ V}^{-1} \text{ s}^{-1}$, respectively. The ZnO layer was grown on the *p*-GaN using MBE, and the substrate temperature for the growth of ZnO was kept at 500 °C. After that, an oxide layer was introduced on the *p*-GaN surface by annealing the *p*-GaN/n-ZnO structure in O₂ ambient at 650 °C for 30 min. Metallic Au layer with a diameter of 0.4 mm was deposited onto the GaN and ZnO layers as electrodes by thermal evaporation method.

The electrical properties of the GaN films were measured by a Lakeshore 7707 Hall system. The chemical bonding state of the GaN was characterized using a Thermo Scientific ESCALAB 250 X-ray photoelectron spectroscope (XPS) with an Al K α ($h\nu = 1486.6 \text{ eV}$) line as the irradiation source. Current–voltage (*I*–*V*) characteristics of the Au/GaO_x/*p*-

GaN/*n*-ZnO structures were recorded using an Agilent B1500A semiconductor analyzer. Electroluminescence (EL) measurements of the structures were carried out in a Hitachi F4500 spectrometer. All the tests were performed at room temperature.

ASSOCIATED CONTENT

Supporting Information

The Supporting Information is available free of charge on the ACS Publications website at DOI: 10.1021/acsp Photonics.7b01310.

Figures S1 and S2 (PDF).

AUTHOR INFORMATION

Corresponding Authors

*E-mail: shanx@ciomp.ac.cn.

*E-mail: shendz@ciomp.ac.cn.

ORCID

Chongxin Shan: 0000-0003-2113-5839

Mingming Jiang: 0000-0003-1784-582X

Notes

The authors declare no competing financial interest.

ACKNOWLEDGMENTS

This work was financially supported by the National Natural Science Foundation of China (U1604263 and 61604132), and the National Science Foundation for Distinguished Young Scholars of China (61425021).

REFERENCES

- (1) Ju, Z. G.; Liu, W.; Zhang, Z. H.; Tan, S. T.; Ji, Y.; Kyaw, Z.; Zhang, X. L.; Lu, S. P.; Zhang, Y. P.; Zhu, B. B. Advantages of the Blue InGaN/GaN Light-Emitting Diodes with an AlGaIn/GaN/AlGaIn Quantum Well Structured Electron Blocking Layer. *ACS Photonics* **2014**, *1* (4), 377–381.
- (2) Piprek, J. Efficiency droop in nitride-based light-emitting diodes. *Phys. Status Solidi A* **2010**, *207* (10), 2217–2225.
- (3) Tan, S. T.; Sun, X. W.; Demir, H. V.; Denbaars, S. P. Advances in the LED Materials and Architectures for Energy-Saving Solid-State Lighting Toward “Lighting Revolution.” *IEEE Photonics J.* **2012**, *4* (2), 613–619.
- (4) Zhang, G.; Guo, X.; Ren, F. F.; Li, Y.; Liu, B.; Ye, J.; Ge, H.; Xie, Z.; Zhang, R.; Tan, H. H. High-brightness polarized green InGaIn/GaN light-emitting diode structure with Al-coated p-GaN grating. *ACS Photonics* **2016**, *3* (10), 1912.
- (5) Ponce, F. A.; Bour, D. P. Nitride-based semiconductors for blue and green light-emitting devices. *Nature* **1997**, *386* (6623), 351–359.
- (6) Sarau, G.; Heilmann, M.; Latzel, M.; Christiansen, S. Disentangling the effects of nanoscale structural variations on the light emission wavelength of single nano-emitters: InGaIn/GaN multiquantum well nano-LEDs for a case study. *Nanoscale* **2014**, *6* (20), 11953.
- (7) Guan, N.; Dai, X.; Messanvi, A.; Zhang, H.; Yan, J.; Gautier, E.; Bougerol, C.; Julien, F. H.; Durand, C.; Eymery, J. Flexible White Light Emitting Diodes Based on Nitride Nanowires and Nanophosphors. *ACS Photonics* **2016**, *3* (4), 597–603.
- (8) Tchoe, Y.; Jo, J.; Kim, M.; Heo, J.; Yoo, G.; Sone, C.; Yi, G. C. Variable-color light-emitting diodes using GaN microdonut arrays. *Adv. Mater.* **2014**, *26* (19), 3019.
- (9) Shi, Z.; Wu, D.; Xu, T.; Zhang, Y.; Zhang, B.; Tian, Y.; Li, X.; Du, G. Improved Electrical Transport and Electroluminescence Properties of p-ZnO/n-Si Heterojunction via Introduction of Patterned SiO₂ Intermediate Layer. *J. Phys. Chem. C* **2016**, *120* (8), 4504.

- (10) Shi, Z. F.; Xu, T. T.; Wu, D.; Zhang, Y. T.; Zhang, B. L.; Tian, Y. T.; Li, X. J.; Du, G. T. Semi-transparent all-oxide ultraviolet light-emitting diodes based on ZnO/NiO-core/shell nanowires. *Nanoscale* **2016**, *8* (19), 9997.
- (11) Fan, Z. Y.; Lin, J. Y.; Jiang, H. X. III-nitride micro-emitter arrays: Development and applications. *J. Phys. D: Appl. Phys.* **2008**, *41* (9), 94001–94012.
- (12) Zhang, S.; Gong, Z.; Mckendry, J. J. D.; Watson, S.; Cogman, A.; Xie, E.; Tian, P.; Gu, E.; Chen, Z.; Zhang, G. CMOS-Controlled Color-Tunable Smart Display. *IEEE Photonics J.* **2012**, *4* (5), 1639–1646.
- (13) Liu, Z.; Chong, W. C.; Wong, K. M.; Lau, K. M. GaN-based LED micro-displays for wearable applications. *Microelectron. Eng.* **2015**, *148* (C), 98–103.
- (14) Day, J.; Li, J.; Lie, D. Y. C.; Bradford, C.; Lin, J. Y.; Jiang, H. X. III-Nitride full-scale high-resolution microdisplays. *Appl. Phys. Lett.* **2011**, *99* (3), 42.
- (15) Sun, Y.; Lu, J.; Ai, C.; Wen, D.; Bai, X. Multilevel resistive switching and nonvolatile memory effects in epoxy methacrylate resin and carbon nanotube composite films. *Org. Electron.* **2016**, *32*, 7–14.
- (16) He, C.; Shi, Z.; Zhang, L.; Yang, W.; Yang, R.; Shi, D.; Zhang, G. Multilevel Resistive Switching in Planar Graphene/SiO₂ Nanogap Structures. *ACS Nano* **2012**, *6* (5), 4214.
- (17) Wang, Y.; Liu, Q.; Long, S.; Wang, W.; Wang, Q.; Zhang, M.; Zhang, S.; Li, Y.; Zuo, Q.; Yang, J. Investigation of resistive switching in Cu-doped HfO₂ thin film for multilevel non-volatile memory applications. *Nanotechnology* **2010**, *21* (4), 045202.
- (18) Sarkar, P. K.; Prajapat, M.; Barman, A.; Bhattacharjee, S.; Roy, A. Multilevel resistance state of Cu/La₂O₃/Pt forming-free switching devices. *J. Mater. Sci.* **2016**, *51* (9), 1–8.
- (19) Pan, F.; Gao, S.; Chen, C.; Song, C.; Zeng, F. Recent progress in resistive random access memories: Materials, switching mechanisms, and performance. *Mater. Sci. Eng., R* **2014**, *83* (1), 1–59.
- (20) Wu, S.; Luo, X.; Turner, S.; Peng, H.; Lin, W.; Ding, J.; David, A.; Wang, B.; Van Tendeloo, G.; Wang, J. Nonvolatile Resistive Switching in Pt/LaAlO₃/SrTiO₃ Heterostructures. *Phys. Rev. X* **2013**, *3* (4), 041027.
- (21) Chang, W. Y.; Lin, C. A.; He, H.; Wu, T. B. Resistive switching behaviors of ZnO nanorod layers. *Appl. Phys. Lett.* **2010**, *96* (24), 323.
- (22) Kim, K. H.; Gaba, S.; Wheeler, D.; Cruzalbrecht, J. M.; Hussain, T.; Srinivasa, N.; Wei, L. A Functional Hybrid Memristor Crossbar-Array/CMOS System for Data Storage and Neuromorphic Applications. *Nano Lett.* **2012**, *12* (1), 389.
- (23) Schön, G. Auger and direct electron spectra in X-ray photoelectron studies of zinc, zinc oxide, gallium and gallium oxide. *J. Electron Spectrosc. Relat. Phenom.* **1973**, *2* (1), 75–86.
- (24) Battistoni, C.; Dormann, J. L.; Fiorani, D.; Paparazzo, E.; Viticoli, S. An XPS and Mössbauer study of the electronic properties of ZnCr_xGa_{2-x}O₄ spinel solid solutions. *Solid State Commun.* **1981**, *39* (4), 581–585.
- (25) Cossu, G.; Ingo, G. M.; Mattogno, G.; Padeletti, G.; Proietti, G. M. XPS investigation on vacuum thermal desorption of UV/ozone treated GaAs(100) surfaces. *Appl. Surf. Sci.* **1992**, *56* (3), 81.
- (26) Carin, R.; Deville, J. P.; Werckmann, J. An XPS study of GaN thin films on GaAs. *Surf. Interface Anal.* **1990**, *16* (1–12), 65–69.
- (27) Wang, C. S.; Nieh, C. H.; Lin, T. Y.; Chen, Y. F. Electrically Driven Random Laser Memory. *Adv. Funct. Mater.* **2015**, *25* (26), 4058–4063.
- (28) Zou, X.; Ong, H. G.; You, L.; Chen, W.; Ding, H.; Funakubo, H.; Chen, L.; Wang, J. Charge trapping-detrapping induced resistive switching in Ba_{0.7}Sr_{0.3}TiO₃. *AIP Adv.* **2012**, *2* (3), 2669.
- (29) Yan, Z. B.; Liu, J. M. Coexistence of high performance resistance and capacitance memory based on multilayered metal-oxide structures. *Sci. Rep.* **2013**, *3* (8), 2482.
- (30) Hota, M. K.; Bera, M. K.; Kundu, B.; Kundu, S. C.; Maiti, C. K. A Natural Silk Fibroin Protein-Based Transparent Bio-Memristor. *Adv. Funct. Mater.* **2012**, *22* (21), 4493–4499.
- (31) Fujii, T.; Kawasaki, M.; Sawa, A.; Kawazoe, Y.; Akoh, H.; Tokura, Y. Electrical properties and colossal electroresistance of heteroepitaxial SrRuO₃/SrTi_{1-x}Nb_xO₃ (0.0002 ≤ x ≤ 0.02) Schottky junctions. *Phys. Rev. B* **2007**, *75* (75), 5101.
- (32) Sawa, A.; Fujii, T.; Kawasaki, M.; Tokura, Y. Hysteretic current–voltage characteristics and resistance switching at a rectifying TiPr_{0.7}Ca_{0.3}MnO₃ interface. *Appl. Phys. Lett.* **2004**, *85* (18), 4073–4075.
- (33) Saito, H.; Mineno, Y.; Yuasa, S.; Ando, K. Reducing Schottky barrier height for Fe/n-GaAs junction by inserting thin GaOx layer. *J. Appl. Phys.* **2011**, *109* (7), 1092.
- (34) Fujisaki, Y.; Koga, H.; Nakajima, Y.; Nakata, M.; Tsuji, H.; Yamamoto, T.; Kurita, T.; Nogi, M.; Shimidzu, N. Transparent Nanopaper-Based Flexible Organic Thin-Film Transistor Array. *Adv. Funct. Mater.* **2014**, *24* (12), 1657–1663.
- (35) Ishikawa, H.; Kobayashi, S.; Koide, Y.; Yamasaki, S.; Nagai, S.; Umezaki, J.; Koike, M.; Murakami, M. Effects of surface treatments and metal work functions on electrical properties at p-GaN/metal interfaces. *J. Appl. Phys.* **1997**, *81* (3), 1315–1322.
- (36) Yang, J. B.; Chang, T. C.; Huang, J. J.; Chen, S. C.; Yang, P. C.; Chen, Y. T.; Tseng, H. C.; Sze, S. M.; Chu, A. K.; Tsai, M. J. Resistive switching characteristics of gallium oxide for nonvolatile memory application. *Thin Solid Films* **2013**, *529* (5), 200–204.
- (37) Zhu, G. Y.; Li, J. T.; Tian, Z. S.; Dai, J.; Wang, Y. Y.; Li, P. L.; Xu, C. X. Electro-pumped whispering gallery mode ZnO microlaser array. *Appl. Phys. Lett.* **2015**, *106* (2), 2230.
- (38) Yang, Q.; Wang, W.; Xu, S.; Wang, Z. L. Enhancing light emission of ZnO microwire-based diodes by piezo-phototronic effect. *Nano Lett.* **2011**, *11* (9), 4012–4017.
- (39) Zhu, G. Y.; Xu, C. X.; Lin, Y.; Shi, Z. L.; Li, J. T.; Ding, T.; Tian, Z. S.; Chen, G. F. Ultraviolet electroluminescence from horizontal ZnO microrods/GaN heterojunction light-emitting diode array. *Appl. Phys. Lett.* **2012**, *101* (4), 2720.
- (40) Lu, Y. J.; Shi, Z. F.; Shan, C. X.; Shen, D. Z. ZnO-based deep-ultraviolet light-emitting devices. *Chin. Phys. B* **2017**, *26* (4), 50–58.